UDC 551.509.313 : 519.28

NOTE ON THE ACCUMULATED ERROR IN THE NUMERICAL INTEGRATION OF A SIMPLE FORECAST MODEL

WALTER JAMES KOSS

National Hurricane Research Laboratory, ESSA, Miami, Fla.

ABSTRACT

A linearized, two-level forecast model with known analytic solution is numerically integrated to examine the behavior of the accumulated error (truncation and machine word "round-off" error). The results indicate that for linear models numerically integrated with centered differences: 1) the ratio of space increment to disturbance wavelength that yields sufficient accuracy in a reasonable amount of computation real time is on the order of 10^{-1} to 10^{-2}; 2) the largest time increment consistent with the stability criterion should be used for computation expediency.

Computations performed on computers having different word lengths did not yield significant differences in the results for this model integrated out to 7 days.

1. INTRODUCTION

The stability and accuracy of various finite-difference approximations to differential equations encountered in fluid dynamics problems have been investigated by various authors. The reader is directed to the work of Richtmyer (1962, 1957), Fischer (1965), Lilly (1965), Kurihara (1965), Phillips (1960), Molenkamp (1968), Crowley (1968), Kasahara (1965), Holton (1967), and Young (1968) for a detailed overview of the difference forms encountered in meteorological problems. Forsythe and Wasow (1960) present an excellent introduction to the general mathematical problem.

In this paper, we examine the accumulated error incurred during the time integration of a linearized, two-level forecast model that has a known analytic solution. The accumulated error at a given time is defined as the difference between the analytic and the numerical solutions and is produced by both truncation and round-off (machine word-size truncation). Integrations were performed with various values of the space and time increments and with different machine word lengths in order to determine 1) the importance of varying Δt with fixed Δs (providing the stability criterion is met) in terms of reducing the accumulated error and 2) the relative effects of truncation error versus round-off error in the accumulated error.

2. THE FORECAST MODEL

The numerical model forecasts the perturbation wind shear and geopotential thickness for the 750- to 250-mb layer over a 2000-km square bounded on the south by the Equator. The analytic equations govern linear, nonviscous, adiabatic, quasi-hydrostatic β-plane flow on a stagnant base state. For a detailed description of the model, the equations, and their solutions, see Rosenthal (1965) and Koss (1967). The vertical structure of the model is given in figure 1. The model equations are

$$\frac{\partial \hat{u}}{\partial t}-\beta y\hat{v}+\frac{\partial \hat{\phi}}{\partial x}=0, \tag{1a}$$

$$\frac{\partial \hat{v}}{\partial t}+\beta y\hat{u}+\frac{\partial \hat{\phi}}{\partial y}=0, \tag{1b}$$

and

$$\frac{\partial \hat{\phi}}{\partial t}+\frac{p_2^2\bar{\sigma}_2}{2}\left(\frac{\partial \hat{u}}{\partial x}+\frac{\partial \hat{v}}{\partial y}\right)=0 \tag{1c}$$

where

$$\hat{u}=u_1-u_3,$$
$$\hat{v}=v_1-v_3,$$
and
$$\hat{\phi}=\phi_1-\phi_3; \tag{2}$$

u_k, v_k are the wind velocity components at level k. ϕ_k is the geopotential of the kth pressure level, $p_2=50$ cb. $\bar{\sigma}_2 = 3$ mts units (section 3) is the mean static stability, $\beta=\partial f/\partial y$, where f is the Coriolis parameter, y is distance north from the Equator, and x is east-west distance measured positive eastward. Equation (1c) was obtained by discretizing the continuity and thermodynamic equations in the vertical and combining the two resulting equations. Here, $\omega_0=\omega_4=0$ was used as a boundary condition. A solution (see Koss, 1967, for details) is given by

$$\hat{u}=\hat{v}_{max}\frac{[\gamma^2-(c+\gamma)\beta y^2]}{k(c^2-\gamma^2)}\left(\frac{\beta}{\gamma}\right)^{1/2}e^Y \sin k(x-ct), \tag{3a}$$

$$\hat{v}=\hat{v}_{max}y\left(\frac{\beta}{\gamma}\right)^{1/2}e^Y \cos k(x-ct), \tag{3b}$$

and

$$\hat{\phi}=\hat{v}_{max}\frac{[c\gamma-(c+\gamma)\beta y^2]}{k(c^2-\gamma^2)}(\beta\gamma)^{1/2}e^Y \sin k(x-ct) \tag{3c}$$

where

$\gamma^2=\frac{p_2^2\bar{\sigma}_2}{2}$, $k=\frac{2\pi}{L}$, $Y=\frac{1}{2}\left(1-\frac{\beta y^2}{\gamma}\right)$, and L is the wavelength.

The c is the phase speed of the meteorologically significant solution which is obtained by solving the frequency equation

$$c^3-\frac{1}{k^2}[k^2\gamma^2+\gamma\beta+2\alpha\beta\gamma]c-\frac{\gamma^2\beta}{k^2}=0$$

with $\alpha=1$. This particular solution gives a meridional

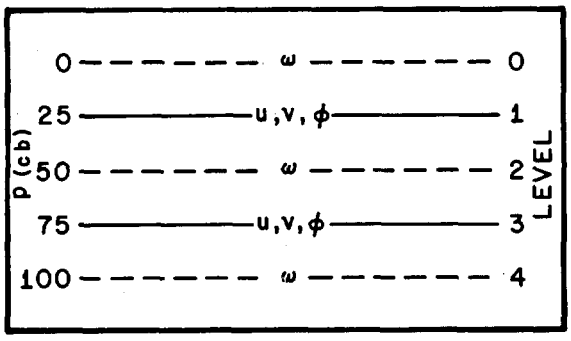

FIGURE 1.—Vertical structure of the model; u, v, and ϕ are defined at levels 1 and 3; $\omega=dp/dt$ is defined at levels 0, 2, and 4.

perturbation velocity component which is asymmetric about the Equator and tends to zero with increasing distance from the Equator.

The finite-difference scheme used in the integrations was the familiar centered difference (leapfrog) scheme which has the following well-known properties:

(I) conditional computational stability,
(II) no changes in wave amplitude result from the integration,
(III) fictitious changes in phase speed occur during the integration,
(IV) splitting of solutions at alternate time steps due to the presence of the "computational" mode introduced by the use of a second-order approximation to a first-order derivative (Kurihara, 1965, and page 73 of Phillips, 1960), and
(V) the uncoupling of solutions of a linear system of equations at alternate time steps due to the use of centered difference approximations to both the space and time derivatives (Platzman, 1958).

Property (V) does not manifest itself in this study since the equations are coupled at alternate time steps through the Coriolis terms.

The "leapfrog" difference analog of equations (1a, b, and c) is

$$\hat{u}^{n+1}_{i,j}=\hat{u}^{n-1}_{i,j}+2\Delta t\left[\beta y_i\hat{v}^{n}_{i,j}-\frac{(\hat{\phi}^{n}_{i,j+1}-\hat{\phi}^{n}_{i,j-1})}{2\Delta s}\right], \quad (4a)$$

$$\hat{v}^{n+1}_{i,j}=\hat{v}^{n-1}_{i,j}-2\Delta t\left[\beta y_i\hat{u}^{n}_{i,j}+\frac{(\hat{\phi}^{n}_{i+1,j}-\hat{\phi}^{n}_{i-1,j})}{2\Delta s}\right], \quad (4b)$$

and

$$\hat{\phi}^{n+1}_{i,j}=\hat{\phi}^{n-1}_{i,j}-\frac{\Delta t}{\Delta s}\gamma^2[\hat{u}^{n}_{i,j+1}-\hat{u}^{n}_{i,j-1}+\hat{v}^{n}_{i+1,j}-\hat{v}^{n}_{i-1,j}] \quad (4c)$$

where Δs is the space increment in both the x (j) and y (i) directions and Δt is the time increment. A forward time difference set of equations is used to initiate the integrations.

3. RESULTS

The following values of parameters were used in all of the integrations:

$L=2000$ km,
$c=-2.0827$ m sec^{-1},
$\beta=2.2865\times10^{-11}$ (m sec)$^{-1}$,
$\hat{v}_{max}=5$ m sec^{-1}, and
$\bar{\sigma}=3$ mts units.

The initial fields of $\hat{u}$, $\hat{v}$, and $\hat{\phi}$ were computed using equations (3a, b, and c) with $t=0$. During the integrations 1) cyclic continuity was used in computing the tendencies at the east-west boundaries (which is reasonable since the solutions are neutral waves) and 2) the tendencies at the north-south boundaries were computed from the analytic expressions to avoid using one-sided space differences.

The integrations are divided into two sets: the first set was obtained on a computer having a 36-bit binary word and the second from a 32-bit (hexadecimal) word. All integrations were performed in normalized floating-point arithmetic. Table 1 gives the accuracy characteristic of these word sizes.

TABLE 1.—*Comparison of the floating-point format of the 32- and 36-bit word used in the numerical integrations. S refers to a single precision word, D refers to a double precision word.*

	36-bit word	32-bit word
Characteristic	7-bit S	7-bit S 7-bit D
Mantissa	28-bit S	24-bit - 6 hexadecimal digit S 56-bit - 14 hexadecimal digit D
Significance (decimal)	~9-digit S	~7.2-digit S ~16.8-digit D

The measure of the accumulated error used here is the root-mean-square error (RMSE) given by

$$\left\{\frac{1}{I^*J}\left[\sum_{i=1}^{I}\sum_{j=1}^{J}(F_{i,j}-F^*_{i,j})^2\right]\right\}^{1/2}$$

where $F_{i,j}$ is the value of the analytic solution at the (i,j)th grid point, $F^*_{i,j}$ is the result of the time integration at the same point, and I^*J is the total number of grid points.

THE INTEGRATIONS IN SET 1

Table 2 lists the RMSE of the $\hat{\phi}$ field (in meters) at the end of 12-hr forecast periods up to 72 hr and percentage errors at the 12- and 72-hr elapsed times. Δs was varied from 40 km to 250 km[1] and Δt was varied from 225 sec to an appropriate upper limit which satisfied the approximate computational stability criterion

$$\left|U\frac{\Delta t}{\Delta s}\right|<1.$$

[1] Forty kilometers was the smallest allowable value of Δs because of computer memory restrictions on a 32K-36-bit word computer without peripherals, that is, tapes, discs, etc. Approximately 28K words were available for the program and variable storage.

TABLE 2.—*RMSE of the $\hat{\phi}$ field (in meters) at the end of 12-hr forecast periods and percentage error of the $\hat{\phi}$ field at the end of 12 hr and 72 hr. The percentage error is defined as the ratio of the RMSE to the average value of the amplitude of $\hat{\phi}$ with a value of 3.4 m and is listed following the RMSE. The bracketed quantity in the Δt column is the number of time steps needed for a 72-hr forecast using that value of Δt. The bracketed quantity with Δs is the total number of grid points in the 2000-km square region using that value of Δs.*

Δt (sec)	Elapsed time (hr)					
	12	24	36	48	60	72
			Δs=250 km [81]			
3600 [72]	.91977 27.	13.9 (409%)	259.	5. × 10^4	9. × 10^7	2. × 10^{11}
2400 [108]	.45351 13.3	.51657	.41766	.66503	.48026	.69119 20.3
1800 [144]	.43677 12.8	.54985	.38438	.59349	.49279	.60916 17.9
900 [288]	.41891 12.3	.56610	.35459	.53203	.59469	.55990 16.5
450 [576]	.41424 12.2	.56791	.35223	.52029	.61878	.54152 15.9
			Δs=125 km [289]			
1200 [216]	.11706 3.4	.10450	.11163	.15693	.15435	.18309 5.4
900 [288]	.11638 3.4	.10709	.10975	.16184	.15038	.19021 5.6
450 [576]	.11570 3.4	.10961	.10832	.16558	.14593	.19485 5.7
225 [1152]	.11552 3.4	.11023	.10797	.16641	.14475	.19540 5.7
			Δs=62.5 km [1089]			
600 [432]	.029845 0.87	.025132	.030313	.038035	.041705	.043266 1.27
450 [576]	.029804 0.87	.025325	.030071	.038379	.041527	.043791 1.28
225 [1152]	.029768 0.87	.025516	.029850	.038715	.041340	.044279 1.30
			Δs=40 km [2601]			
400 [648]	.012327 0.36	.010226	.012694	.015496	.017408	.017627 0.51
225 [1152]	.012316 0.36	.010281	.012628	.015596	.017355	.017755 0.52

Since the system will support inertia-gravity waves having a phase speed of approximately ± 65 m sec^{-1} (L=2000 km), the largest value of Δt used satisfied the criteria with U=75 m sec^{-1}. One integration was performed where the stability criterion was violated (Δs=250 km, Δt=3600 sec). In this case, the RMSE is about twice the maximum value of $\hat{\phi}$ after only 24 time steps.

For each integration, we note an oscillation in the values of the RMSE with time; but in general, the error is increasing with time. The error increase with time can be attributed to the cumulative error. The possible causes of the oscillation will be discussed in a following paragraph.

With Δs fixed, the RMSE both increases and decreases with Δt, depending on which elapsed time column one examines. Since amplitudes are invariant with time (property (II) of the differencing scheme), the data in table 2 suggest that one is probably better off by choosing the largest possible Δt which satisfies the stability criterion, since there may not be a reduction of the accumulated error associated with a reduction of the time-scale truncation error. Gates (1959) has shown for the centered difference form of the linearized barotropic vorticity equation that after the initial time steps the average phase speed of the computed solution can be expressed as a function of Δt and Δs. For values of the parameters used here, the change in phase speed (as computed from equation (76) by Gates (1959)) with respect to Δt is extremely small. Under the assumption that the computed solution phase speed for the system (4a, b, and c) behaves in a similar manner, we conclude that the phenomenon described in the first sentence of this paragraph is not related to property (III). The reason for this behavior will become apparent in the discussion of the 7-day integrations.

Since the differencing scheme is second order, the truncation error is on the order of the square of the normalized space increment. Therefore, halving Δs reduces the truncation error by one-fourth. From the values in the 72-hr column, we see that the percentage error behaves in a similar way as Δs is reduced.

The RMSE for the $\hat{u}$ and $\hat{v}$ fields exhibit the same overall behavior as that of the $\hat{\phi}$ field; hence, those results are not shown here.

Several 7-day integrations were performed with fixed $\lambda=\Delta t/\Delta s$=.0096 for Δs=40, 62.5, 125, and 250 km. The results are shown in figure 2 where the RMSE has been plotted at every time step for the Δs=250-km and 125-km

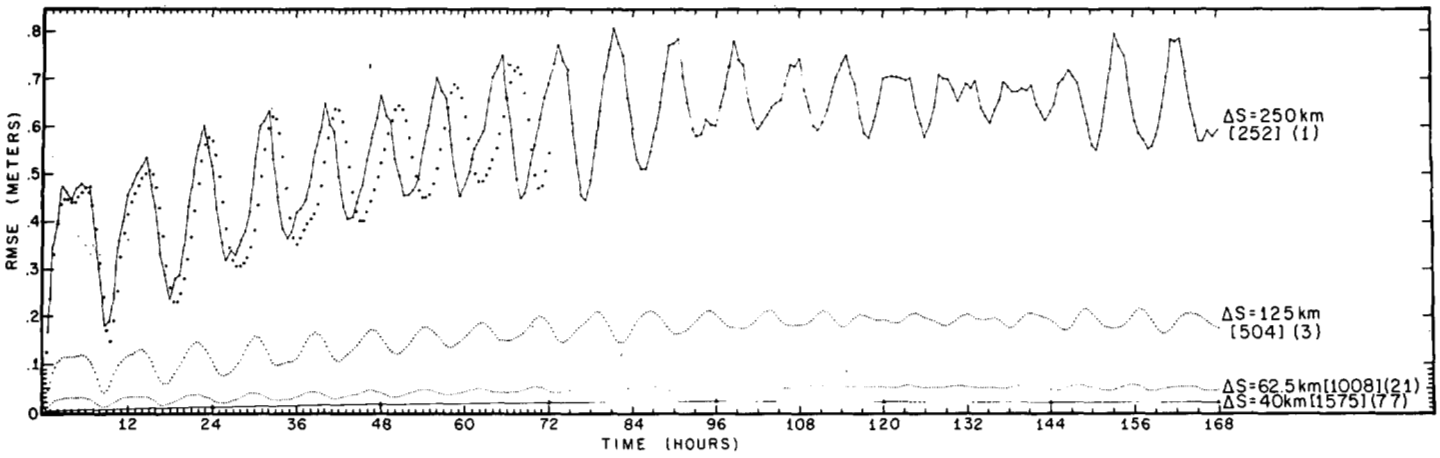

FIGURE 2.—RMSE (in meters) for 7-day integrations, with $\lambda=\Delta t/\Delta s=$ constant for various values of Δs, and for a 3-day integration with $\Delta s=250$ km, $\Delta t=450$ sec (the data points are given by circles). Every time step has been plotted for the 7-day $\Delta s=250$-km and 125-km cases. Alternate time steps are plotted for the $\Delta s=62.5$-km case. The results for the 24-hr forecast periods are given for the $\Delta s=$ 40-km case. For the 3-day forecast, the data are plotted at half-hourly intervals. The boxed quantity is the number of time steps needed to complete the 7-day forecast. The bracketed quantity is the relative real time of the integration with the $\Delta s=250$-km case assigned the base value of 1. (The lines joining the data points have no physical significance.)

cases, at alternate time steps for the $\Delta s=62.5$-km case, and at 24-hr intervals for the $\Delta s=40$-km case. Also shown in the figure are the number of time steps and the relative time needed to complete the integration with the 250-km case assigned the base value of 1. For this forecast period, the reduction of space truncation error is still the important factor in reducing the accumulated error. Here the space/time increments are large enough so that truncation can be considered the major contributor to the error, that is, the round-off error incurred in the many space/time arithmetic operations is not yet dominant. The graphs for the 250-, 125-, and 62.5-km cases exhibit the time oscillation which was suggested by the data in table 2. At first thought, one is tempted to attribute the oscillation to the effect of property (III) of the leapfrog scheme, but there is another explanation for this behavior. Although the initial conditions were given in terms of the meteorologically important wave ($c=-2.0827$ m sec^{-1}), the computational system will support inertia-gravity waves as does the analytic system. The phase speed of these waves (for $L\leq 5000$ km) is on the order of ± 70 m sec^{-1}, which gives a period of about 8 hr. The oscillations in the RMSE graphs have a period of approximately 8 hr which is independent of both Δs and Δt. The independence from Δt is shown by the plot of the $\Delta s=250$ km and $\Delta t=450$ sec 72-hr forecast data, which has the same period as the $\Delta s=250$ km and $\Delta t=2400$ sec forecast data. This suggests that the errors generated in the initial time steps excite the inertia-gravity waves which then propagate through the system. The use of a small Δt only delays the excitation (here there is a lag of about 1 hr for the two compared cases), since it takes longer for the smaller truncation error to accumulate.

There is the possibility that the error caused by the computational change of phase speed is not revealed by the RMSE, which would be the case if the phase speed error is very small. But, if the analytic wave and computational wave become more out-of-phase as the forecast progresses, this error would manifest itself as a monotonic increase in the RMSE. Also, there is no indication throughout the forecast period that property (IV) of the leapfrog scheme (the solution splitting at alternate time steps) has occurred. This phenomenon could also be hidden by the RMSE, through the squaring of the error in the formation of the RMSE.

THE INTEGRATIONS IN SET 2

Three 7-day integrations were performed on a computer having a 32-bit word. Of these, one intergration was computed using double precision-type arithmetic (64-bit word). In all three integrations the analytic data were computed in double precision. This allows a comparison of these results with those computed with the 36-bit word. Table 3 shows the RMSE for the $\hat{\phi}$ fields (in these computations $\lambda=.0096$). Here, the last digit in the 36-bit word result was obtained by rounding off the stored number for output display. All digits of the 32- and 64-bit words are certain (table 1); to compare the results with those of the 36-bit word, use the usual rounding convention when rounding to six (or five) digits. The differences in the results are insignificant. We must keep in mind that these results apply for a linear model; a similar experiment with a complex nonlinear system could possibly yield the opposite conclusion.

4. REMARKS

During the course of the computations reported on in this paper, we were not concerned primarily with the question of the stability and accuracy of the finite-differ-

TABLE 3.—*RMSE of the $\hat{\phi}$ field (in meters) computed on a 32-bit word computer in single and in double precision arithmetic and on a 36-bit word computer. Time is the elapsed forecast time in hours. For these computations, $\lambda=\Delta t/\Delta s=$ constant.*

Time (hr)	$\Delta s=40$ km		$\Delta s=125$ km		
	32-bit word	36-bit word	32-bit word	64-bit word	36-bit word
12			.11705 89	.11705 88	.11706
24	.010225 60	.010225	.10449 92	.10449 91	.10450
36			.11163 30	.11163 29	.11163
48	.015507 72	.015507	.15692 59	.15692 56	.15693
60			.15435 56	.15435 53	.15435
72	.017635 46	.017634	.18309 31	.18309 27	.18309
84			.17208 68	.17208 69	.17209
96	.020381 05	.020379	.20326 68	.20326 62	.20327
108			.18195 96	.18195 91	.18196
120	.020659 76	.020659	.19120 75	.19120 72	.19121
132			.20379 57	.20379 54	.20380
144	.019077 01	.019074	.19149 46	.19149 30	.19149
156			.20765 61	.20765 59	.20765
168	.019412 13	.019411	.17597 78	.17597 70	.17598

ence scheme used in integrating the system of differential equations. Instead, we considered the practical aspect of the problem, that is, the interrelation of truncation error and round-off error in the error accumulated during the integration. The model, being linear and free of diabatic and viscous effects, allows verification of the integrations to within the machine accuracy of the computed values of the analytic solutions. Therefore, one is able to associate the overall behavior of the error with changes in the space/time parameters. The error incurred by evaluating the analytic expressions for the tendencies on the north and south boundary is a maximum when Δt is large, and this is when the truncation error is at a maximum over the entire grid. The effects of this error are, therefore, secondary in the overall evaluation.

The rate of error accumulation is strongly dependent upon the complexity of the physical system being examined. Here, although the model is linear and basically simple, it is determined by a system of three equations, one of which is strongly space-increment dependent: the $\hat{\phi}$ tendency is given by the horizontal divergence of the perturbation wind shear. This computation is an excellent source of truncation error.

Several conclusions concerning the computer application of the leapfrog scheme can be made based on these integrations:

1) For a given value of the space increment, one should choose the largest value of the time increment consistent with the stability criterion. The use of a smaller value of Δt does not always guarantee a reduction of the accumulated error even though the theoretical truncation error in the time scale is reduced. The additional computations needed with a smaller Δt will usually introduce compensating round-off errors. More important is the effect of the excited gravity waves which may be supported by the system. The lag in the oscillation of the error curves caused by changes in Δt can give results as those given in table 2: the "goodness" of the smaller Δt depends on the forecast period examined. Hence, the space truncation is the important factor in the error accumulation.

2) Once the characteristic scale (L) of the motions being studied has been determined, there is an optimal range of values of the space increment (Δs) in terms of both "acceptable" error accumulation and computer time. Reduction of the magnitude of Δs will reduce the accumulated error because of the reduction in both the space- and time-scale truncation error. But extremely small values of Δs yield rapid accumulation of round-off error which will dominate the truncation error.[2] This phenomenon is a function of the computer word size and the total number of arithmetic operations in the computation. Inspection of table 3 shows that this was not the case here for either word size. Figure 2 shows that the slight gain in accuracy made in going from $\Delta s=62.5$ km to $\Delta s=40$ km was at the expense of a three-fold increase in computer running time. If $h=\Delta s/L$, then $h=0.03$, for this experiment yields less than a 2 percent average error in the $\hat{\phi}$ field in a reasonable amount of computing time. As mentioned above, that the round-off error was not dominant in the examined cases is shown by comparing the results of the single precision and double precision computations. Round-off error would become evident in the accumulated error for values of Δs much smaller than 40 km, that is, for $h<<0.02$, through an increase in the percentage error of the $\hat{\phi}$ fields as Δs decreases. The small percentage errors for $h\sim0.03$ and the large amounts of computation needed for integrations with smaller values of h are justification for not performing the computations with $\Delta s<40$ km.

Modifying the governing equations by the addition of nonlinear advection, viscous effects, and diabatic effects would not alter the magnitude of the truncation error if the same finite-difference approximations are used, but the round-off error possibly could be greatly increased. (We are assuming that the system remains computationally stable with the addition of terms.)

In general, one could use the same technique employed here in other problems to determine feasible choices of integration parameters, regardless of the existence or nonexistence of comparison analytic solutions to the problem at hand. The choice of space increment can be established by noting the relative change in the computed field variable for a short forecast period as the grid is modified from a coarse to a fine one. (The stability criterion determines the time increments, therefore the number of time steps required.) As table 2 demonstrates for the problem considered here, the magnitude of the error is roughly determined in relatively few time steps. Hence, knowledge of the absolute error is not absolutely necessary.

From a few preliminary "dry" runs (in which viscous and diabatic effects can be suppressed) the "optimal"

[2] This can be amply demonstrated by numerically integrating the ordinary differential equation $dy/dx=y$, $y(x=0)=1$, over the interval [0, 1], allowing $h=\Delta x$ to vary from 10^{-1} to 10^{-6} and graphing the error at $x=1$ against the step size h.

space increment can be chosen on the basis of 1) computer economics (running times and memory requirements), and more importantly, 2) the physical reality of the results. The addition of forcing functions to the equations could possibly alter the stability properties of the system and require a change in the value of the space increment. The dry run equations define a physical system whose behavior can be qualitatively diagnosed from the equations. The numerical results of the dry run should concur with the qualitative reasoning when suitable values of the parameters are used in the integration.

REFERENCES

Crowley, W. P., "Numerical Advection Experiments," *Monthly Weather Review*, Vol. 96, No. 1, Jan. **1968**, pp. 1–11.

Fischer, G., "A Survey of Finite-Difference Approximations to the Primitive Equations," *Monthly Weather Review*, Vol. 93, No. 1, Jan. **1965**, pp. 1–10.

Forsythe, G. E., and Wasow, W. R., *Finite Difference Methods for Partial Differential Equations*, John Wiley and Sons, Inc., New York, **1960**, 444 pp.

Gates, W. L., "On the Truncation Error, Stability, and Convergence of Difference Solutions of the Barotropic Vorticity Equation," *Journal of Meteorology*, Vol. 16, No. 5, Oct. **1959**, pp. 556–568.

Holton, J. R., "A Stable Finite Difference Scheme for the Linearized Vorticity and Divergence Equation System," *Journal of Applied Meteorology*, Vol. 6, No. 3, June **1967**, pp. 519–522.

Kasahara, A., "On Certain Finite-Difference Methods for Fluid Dynamics," *Monthly Weather Review*, Vol. 93, No. 1, Jan. **1965**, pp. 27–31.

Koss, W. J., "Further Theoretical Considerations of Tropospheric Wave Motions in Equatorial Latitudes," *Monthly Weather Review*, Vol. 95, No. 5, May **1967**, pp. 283–297.

Kurihara, Y., "On the Use of Implicit and Iterative Methods for the Time Integration of the Wave Equation," *Monthly Weather Review*, Vol. 93, No. 1, Jan. **1965**, pp. 33–46.

Lilly, D. K., "On the Computational Stability of Numerical Solutions of Time-Dependent Non-linear Geophysical Fluid Dynamics Problems," *Monthly Weather Review*, Vol. 93, No. 1, Jan. **1965**, pp. 11–26.

Molenkamp, C. R., "Accuracy of Finite-Difference Methods Applied to the Advection Equation," *Journal of Applied Meteorology*, Vol. 7, No. 2, Apr. **1968**, pp. 160–167.

Phillips, N. A., "Numerical Weather Prediction," *Advances in Computers*, Vol. 1, Academic Press, New York, **1960**, pp. 43–90.

Platzman, G. W., "A Numerical Computation of the Surge of June 26, 1954 on Lake Michigan," *Geophysica*, Vol. 6, No. 3/4, **1958**, pp. 407–438.

Richtmyer, R. D., *Difference Methods for Initial Value Problems*, Interscience Publishers, New York, **1957**, 238 pp.

Richtmyer, R. D., "A Survey of Difference Methods for Nonsteady Fluid Dynamics," *NCAR Technical Note* 63–2, National Center for Atmospheric Research, Boulder, Colo., **1962**, 25 pp.

Rosenthal, S. L., "Some Preliminary Theoretical Considerations of Tropospheric Wave Motions in Equatorial Latitudes," *Monthly Weather Review*, Vol. 93, No. 10, Oct. **1965**, pp. 605–612.

Young, J. A., "Comparative Properties of Some Time Differencing Schemes for Linear and Nonlinear Oscillations," *Monthly Weather Review*, Vol. 96, No. 6, June **1968**, pp. 357–364.

[*Received May 2, 1969; revised August 13, 1969*]